HAL
open science

Three different Ge environments in a new Sr 5 CuGe 9 O 24 phase synthesized at high pressure and high temperature

Holger Klein, Stéphanie Kodjikian, Rémy Philippe, Lei Ding, Claire Colin, Céline Darie, Pierre Bordet

To cite this version:

Holger Klein, Stéphanie Kodjikian, Rémy Philippe, Lei Ding, Claire Colin, et al.. Three different Ge environments in a new Sr 5 CuGe 9 O 24 phase synthesized at high pressure and high temperature. Acta Crystallographica Section B : Structural Science, Crystal Engineering and Materials [2014-..], 2020, 76 (5), pp.727-732. 10.1107/S2052520620008914 . hal-02941287

HAL Id: hal-02941287

https://hal.science/hal-02941287v1

Submitted on 4 Dec 2020

HAL is a multi-disciplinary open access archive for the deposit and dissemination of scientific research documents, whether they are published or not. The documents may come from teaching and research institutions in France or abroad, or from public or private research centers.

L'archive ouverte pluridisciplinaire **HAL**, est destinée au dépôt et à la diffusion de documents scientifiques de niveau recherche, publiés ou non, émanant des établissements d'enseignement et de recherche français ou étrangers, des laboratoires publics ou privés.

Three different Ge environments in a new $Sr_5CuGe_9O_{24}$ phase synthesized at high pressure and high temperature

Holger Klein[1,2], Stéphanie Kodjikian[1,2], Rémy Philippe[1,2], Lei Ding[1,2+], Claire V. Colin[1,2], Céline Darie[1,2], Pierre Bordet[1,2]
[1]*Univ. Grenoble Alpes, Inst NEEL, F-38042 Grenoble, France*
[2]*CNRS, Inst NEEL, F-38042 Grenoble, France*
[+]*Present address: ISIS Facility, Rutherford Appleton Laboratory, Harwell Oxford, Didcot OX11 0QX, United Kingdom*

Abstract

In the framework of expanding the range of copper-based compounds in the pyroxene family we have synthesized at high pressure and high temperature a powder containing a mixture of a new phase with stoichiometry $Sr_5CuGe_9O_{24}$ with two identified impurity phases. Electron crystallography showed that the new phase crystallizes with a monoclinic structure with cell parameters a = 11.6 Å, b = 8.1 Å, c = 10.4 Å and β = 101° and space group *P2/c*. We applied the recently developed low-dose electron diffraction tomography method to solve the structure by direct methods. The obtained structure model contains all 9 independent cation positions and all 13 oxygen positions. A subsequent refinement against X-ray powder diffraction data ascertained the high quality of the structure solution, in particular the unusual structural arrangement that there are three different environments for Ge in this phase.

Synopsis

The high-pressure high-temperature phase $Sr_5CuGe_9O_{24}$ was solved by low-dose electron diffraction tomography and refined against X-ray powder diffraction data. The Ge ions in this compound have three different coordination numbers.

Keywords: electron crystallography, structure determination, high pressure - high temperature compound, pyroxene

1. Introduction

Compounds of the pyroxene family, that can incorporate all the 3d transition metal elements, have recently drawn a considerable interest thanks to their original and diverse magnetic properties including multiferroism (Jodlauk *et al.*, 2007; Kim *et al.*, 2012; Ding *et al.*, 2016), linear magneto-electric effect (Nénert *et al.*, 2010; Ding *et al.*, 2016b) or quasi-one-dimensional magnetic behavior (Valenti *et al.*, 2002). Such physical properties stem essentially from their unique quasi-one-dimensional crystal structure and the competition between inter- and intra-chain magnetic interactions. Among them, pyroxenes containing spin-½ of Cu^{2+} or Ti^{3+} cations have been found to exclude the magnetic long range ordering but yield exotic quantum ground states and spin excitations due to the presence of strong quantum fluctuations and the orbital ordering such as a spin singlet ground state (Sasago *et al.*, 1995) and spin-Peierls transitions (Isobe *et al.*, 2002).

$CaCuGe_2O_6$ appears to be the first copper-containing pyroxene capturing both the low dimensional feature and the half-spin configuration (Sasago *et al.*, 1995). It has been found to

show a spin-singlet ground state and a finite energy gap between the ground state and excited states (Zheludev *et al*. 1996). To seek for more copper-bearing pyroxenes, we have started investigations on compounds with chemical formulas $MCu^{2+}T_2O_6$ (M = divalent transition metal, T = Si or Ge). Recently, through soft chemistry methods, we have successfully synthesized the $Cu_{0.8}Mg_{1.2}Si_2O_6$ clinopyroxene compound (Ding *et al.*, 2016c) and investigated its detailed crystal structure and magnetic properties. It turns out that $Cu_{0.8}Mg_{1.2}Si_2O_6$ only shows a paramagnetic behavior due to the weak interactions between Cu^{2+} cations in the strongly distorted structure induced by the Jahn-Teller effect. In light of our recent work on the magnetic pyroxene $SrMGe_2O_6$ (M=Co, Mn) (Ding *et al.*, 2016; Colin *et al*., 2020), we have employed various synthesis methods to explore the copper-containing analog.

A sample with the nominal composition $SrCuGe_2O_6$ was synthesized at high pressure (4 GPa) and high temperature (900 °C). However, it can not be identified as a pyroxene phase. X-ray powder diffraction (XRPD) showed a great number of diffraction peaks, which could not be rationally indexed by any known phase, indicating the synthesis of at least one unknown phase. We have therefore undertaken an electron crystallographic analysis of the as-synthesized sample. In this work, we show that the structure of the hitherto unknown phase $Sr_5CuGe_9O_{24}$ can be solved using the low-dose electron diffraction tomography (LD-EDT), a method we have developed recently (Kodjikian *et al.*, 2019). In the previous publication centered on the method we used the structure of $Sr_5CuGe_9O_{24}$ as an example of the validity of the method. We present here the details of the structure solution and refinement, and discuss the structure on a crystal chemical basis.

2. Experimental

2.1. Synthesis

The sample with nominal composition $SrCuGe_2O_6$ was synthesized at high pressure - high temperature conditions in a Belt-type apparatus. A stoichiometric mixture of reagent-grade SrO, CuO, and GeO_2 was sealed in a gold capsule in a glove box. Then the capsule was heated for two hours at 900 °C under a pressure of 4 GPa. The resulting sample consisted of a greenish powder.

2.2. X-ray diffraction

An X-ray powder diffraction pattern was collected for 2θ between 10° and 90° at room temperature on a Bruker D5000 diffractometer in transmission geometry equipped with a linear PSD. The Cu $K_{\alpha 1}$ radiation (λ=1.5406 Å) was selected by a primary Ge(111) focusing monochromator. The Rietveld refinement of the powder pattern was carried out using JANA2006 (Petricek *et al.*, 2014).

2.3. Electron Crystallography

The TEM experiments were carried out on a Philips CM300ST, equipped with a TVIPS F416 CMOS camera, a Nanomegas Spinningstar device and a Bruker Silicon Drift Detector for EDS. The synthesized powder was crushed in an agate mortar and a suspension of the powder in ethanol was deposited on a holey carbon film supported by a gold grid for TEM analysis.

A large number of powder particles were characterized by EDS in order to identify the different phases present in the powder.

The diffraction intensities were measured in the recently developed low-dose electron diffraction tomography method (Kodjikian *et al.*, 2019) on one selected particle. The tilt step between two frames of the tomography was chosen as 1°, the precession angle was 1.25°. A

data set of 100 frames with an exposure time of 0.5 s was recorded from a single particle of approximate sizes of 1 µm * 0.5 µm. During the automated data acquisition the beam was blanked from the sample between the exposures in order to irradiate the crystal only during the exposure time of the diffraction patterns.

3. Results

The XRPD pattern showed a high number of diffraction peaks and no *ab initio* structure solution was possible from this data. Moreover, no known phase could explain all of the diffraction peaks. We therefore had to resort to energy dispersive spectroscopy and electron diffraction in a transmission electron microscope.

3.1. Stoichiometry

Scanning the particles by EDS showed that the powder is a mixture of two minority phases, CuO and Cu_2GeO_4, and a majority phase containing a cation proportion of 7% of Cu, 35% Sr and 58% Ge (oxygen being too light to be properly quantified by EDS). The oxygen stoichiometry can be determined with respect to electroneutrality with the corresponding valences of the precursor materials: Cu^{2+}, Sr^{2+}, Ge^{4+}. From these results we concluded that for the crystal two chemical compositions, $Sr_5CuGe_8O_{22}$ or $Sr_5CuGe_9O_{24}$, were possible. For the structure solution, we took into account both scenarios.

3.2. Structure solution by electron diffraction

The data treatment of the electron diffraction tomography with PETS (Palatinus *et al.*, 2011) and the JANA2006 suite (Petricek *et al.*, 2014) yielded a monoclinic cell (a = 11.8 Å; b = 8.1 Å; c = 10.3 Å; β = 101.3°, V = 984 Å^3) of space group *P2/c*. The complete data set consists of 1916 independent reflections, which represents a completeness of 69 % and a redundancy of 3.1 at a resolution of 0.7 Å.

The structure was then solved by direct methods in SIR2014 (Burla *et al.*, 2015) via the JANA2006 user interface. SIR2014 uses the information of the chemical composition in the structure solution calculations. Since there was no certitude of the chemical composition we had to try structure solutions with both stoichiometries. The best results in terms of interatomic distances and leaving no voids in the structure were obtained with the composition $Sr_5CuGe_9O_{24}$. The obtained structure contained all 9 independent cation positions as well as all 13 independent oxygen positions (see table 1 for peak heights and table 2 for coordinates). In the electron density map calculated by SIR2014 there are clear steps in the peak height between the last cation and the first oxygen position. The final *R*-value was 31%, which is a usual value for structure solutions from electron diffraction data.

Table 1: The peak list output from SIR2014. There is a clear difference in peak height between the cations and the oxygen peaks.

Serial	Atom	Height	Cation-oxygen distance	Newly attributed cation
1)	Sr1	7.06	2.50 Å – 2.70 Å	
2)	Ge1	6.63	2.50 Å – 2.71 Å	Sr
3)	Ge2	6.50	2.41 Å – 2.68 Å	Sr
4)	Sr2	6.02	1.64 Å – 1.89 Å	Ge
5)	Sr3	5.85	1.63 Å – 1.85 Å	Ge

6)	Ge3	5.81	1.70 Å – 1.81 Å	
7)	Ge4	5.49	1.81 Å – 1.93 Å	
8)	Ge5	5.48	1.85 Å – 1.87 Å	
9)	Cu1	4.85	1.86 Å – 1.89 Å	
10)	O1	2.44		
11)	O2	2.21		
12)	O3	2.14		
13)	O4	2.12		
14)	O5	2.12		
15)	O6	2.1		
16)	O7	2.07		
17)	O8	2.03		
18)	O9	1.95		
19)	O10	1.91		
20)	O11	1.84		
21)	O12	1.76		
22)	O13	1.68		

Since SIR2014 doesn't always assign the correct cation to a peak in the electron density map we compared the cation – oxygen distances to those observed in another structure with a similar stoichiometry ($Sr_2CuGe_2O_7$, Tovar *et al.*, 1998). In this structure the cation-oxygen distances are 1.63 Å – 1.76 Å for Ge-O, 1.93 Å for Cu-O and 2.54 Å – 2.74 Å for Sr-O. The forth column of table 1 summarizes the observed cation-oxygen distances and the attributed cations are reported in the last column if this differs from the choice of SIR2014. In the resultant list, the three highest peaks obtained by SIR2014 correspond to the heaviest atoms (Sr), the following five to Ge and the last cation position is occupied by the lightest cation (Cu). The resulting stoichiometry is $Sr_5CuGe_9O_{24}$ which is consistent with the composition determined by the EDS measurement.

The refinement of the structure could have been tempted with the electron diffraction data. However, for such a complex structure containing 22 independent atom positions and a large data set of 100 frames, a full dynamical refinement takes more than 24 hours of calculation time on the standard PC that was available. We therefore opted for a refinement using the already recorded XRPD data.

3.3. XRPD refinement

The structure solved by electron crystallography was then refined using the powder X-ray diffraction data obtained from the mixed powder. The presence of the two minor phases detected by TEM-EDS was confirmed: CuO (monoclinic *C2/c*, *a* = 4.6870(4) Å, *b* = 3.4289(3)

Å, c = 5.1336(5) Å, β = 99.509(6)°) and $CuGe_2O_4$ (tetragonal $I4_1/amd$, a = 5.603559 Å, c = 9.361530 Å). The relative mass proportions of the three phases $Sr_5CuGe_9O_{24}$, CuO and $CuGe_2O_4$ are 0.847(3), 0.084(2) and 0.069(2). For the refinement, a Thomson-Cox-Hastings description of the pseudo-Voigt reflection profiles was used and the background was described by a Legendre polynomial. All positional parameters of the $Sr_5CuGe_9O_{24}$ phase were refined, together with isotropic atomic displacement parameters (a.d.p.). The a.d.p.'s of all the oxygen atoms were constrained to be equal. A plot of the final refinement is shown in figure 1. The refined structural parameters and reliability factors are presented in table 2. The cell parameters are in good agreement with the ones obtained by electron crystallography and the refined atomic positions confirm those obtained in the structure solution.

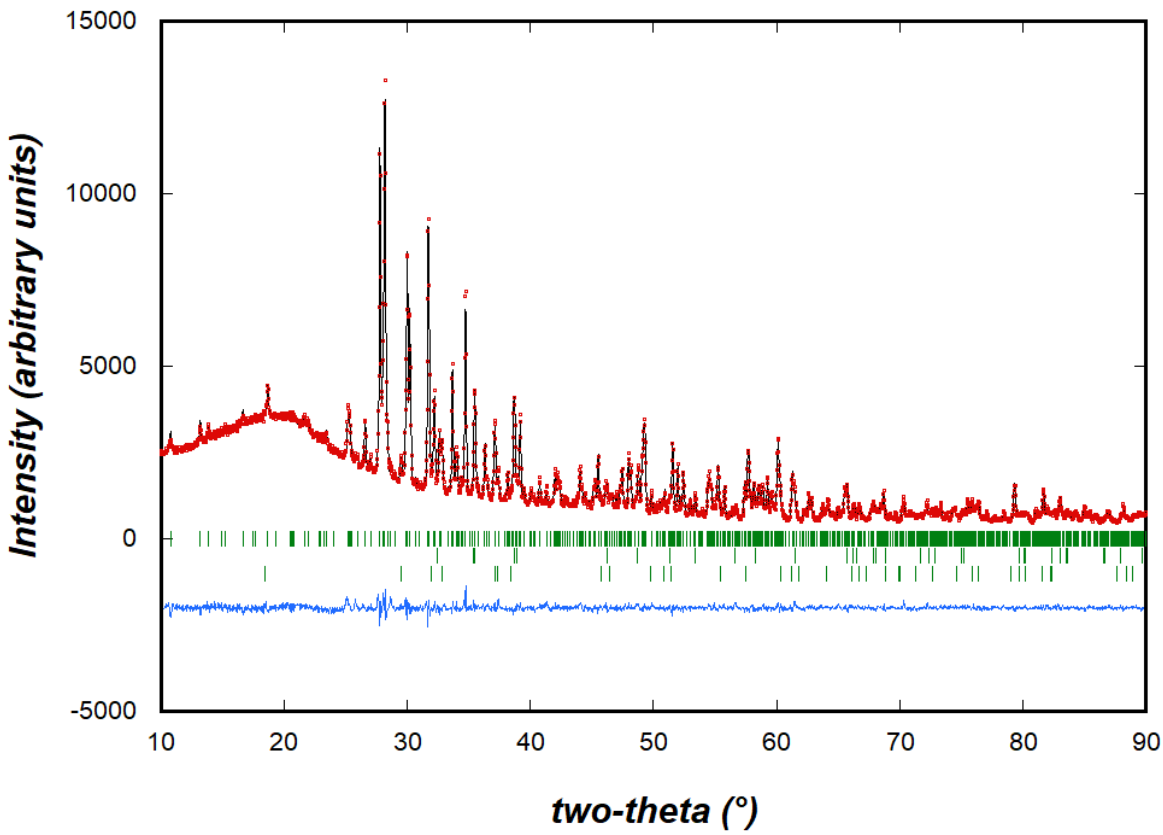

Figure 1: Rietveld plot for the refinement of the XRPD pattern. From top to bottom, the tick marks show the positions of the Bragg reflections for $Sr_5CuGe_9O_{24}$, CuO and $CuGe_2O_4$.

Table 2: Wyckoff positions and coordinates as obtained by the XRPD refinement for $Sr_5CuGe_9O_{24}$ at room temperature. Space group $P2/c$, a = 11.8817(3) Å, b = 8.1928(2) Å, c = 10.3237(2) Å, β = 101.597(13)°. R_p = 2.84, wR_p = 3.76, gof = 1.55, $R_{Bragg}(obs)$ = 6.04 and the initial positions obtained from electron crystallography. The last column shows the distances between the positions.

XRPD				Electron crystallography				Distance
name	x	y	z	name	x	y	z	
Sr1	0	0.3531(8)	0.75	Sr1	0	0.358	0.75	0.040 Å

Sr2	0.7559(4)	0.0316(5)	0.6837(4)	Ge2	0.756	0.031	0.684	0.006 Å
Sr3	0.6505(4)	0.4849(5)	0.6817(5)	Ge1	0.652	0.481	0.678	0.055 Å
Ge1	0.8529(5)	0.7110(6)	0.9356(5)	Sr3	0.854	0.709	0.933	0.036 Å
Ge2	0.5889(4)	0.1750(7)	0.3707(6)	Sr2	0.586	0.173	0.374	0.055 Å
Ge3	0.7896(5)	0.6712(7)	0.4765(5)	Ge3	0.788	0.672	0.476	0.020 Å
Ge4	0.5412(4)	0.8401(7)	0.4122(6)	Ge4	0.543	0.843	0.408	0.057 Å
Ge5	0	0.7801(9)	0.75	Ge5	0	0.775	0.75	0.042 Å
Cu1	0	0	0	Cu1	0	0	0	0.000 Å
O1	0.797(2)	0.695(3)	0.315(3)	O1	0.802	0.7	0.316	0.077 Å
O2	0.544(2)	0.964(3)	0.630(3)	O8	0.541	0.953	0.6	0.314 Å
O3	0.944(2)	0.593(3)	0.827(3)	O2	0.938	0.619	0.847	0.308 Å
O4	0.646(2)	0.675(3)	0.489(3)	O3	0.637	0.675	0.486	0.111 Å
O5	0.415(2)	0.736(3)	0.469(3)	O6	0.419	0.749	0.48	0.160 Å
O6	0.671(2)	0.977(3)	0.421(3)	O7	0.665	0.976	0.403	0.181 Å
O7	0.5	0.344(5)	0.25	O4	0.5	0.321	0.25	0.192 Å
O8	0.910(2)	0.818(3)	0.065(3)	O9	0.901	0.845	0.052	0.270 Å
O9	0.869(2)	0.784(3)	0.595(3)	O5	0.862	0.798	0.605	0.184 Å
O10	0.716(2)	0.724(3)	0.836(3)	O11	0.71	0.737	0.846	0.181 Å
O11	0.817(2)	0.527(3)	0.026(2)	O10	0.817	0.532	0.03	0.060 Å
O12	0.5	0.740(4)	0.25	O12	0.5	0.74	0.25	0.001 Å
O13	0.909(2)	0.921(3)	0.820(3)	O13	0.915	0.915	0.839	0.199 Å

4. Discussion

In a powder containing 3 different phases we have solved a complex structure by low-dose electron diffraction tomography. The obtained model contained all the atoms of the structure including all light oxygen ones. In the electron density map obtained by SIR the highest peaks correspond to the heaviest cations and there is a clear distinction between the cations and the anions.

Even though the chemical species of the cations are not all correctly attributed by SIR, the peak heights reflect the correct order with the highest peaks corresponding to Sr which is the heaviest cation followed by the Ge ions and finally the lightest cation, namely Cu. This observation is corroborated by the cation – oxygen distances and led to the attribution of the chemical species to the cation positions that were subsequently confirmed by the XRPD refinement.

The high quality of the structure solution is established when comparing the atom positions to the ones refined with the XRPD data (last column of table 2). The distances of the cations in the first solution to the refined positions are between 0 Å and 0.057 Å, with an average of 0.035 Å. The oxygen positions show differences between 0.001 Å and 0.314 Å, with an average of 0.172 Å.

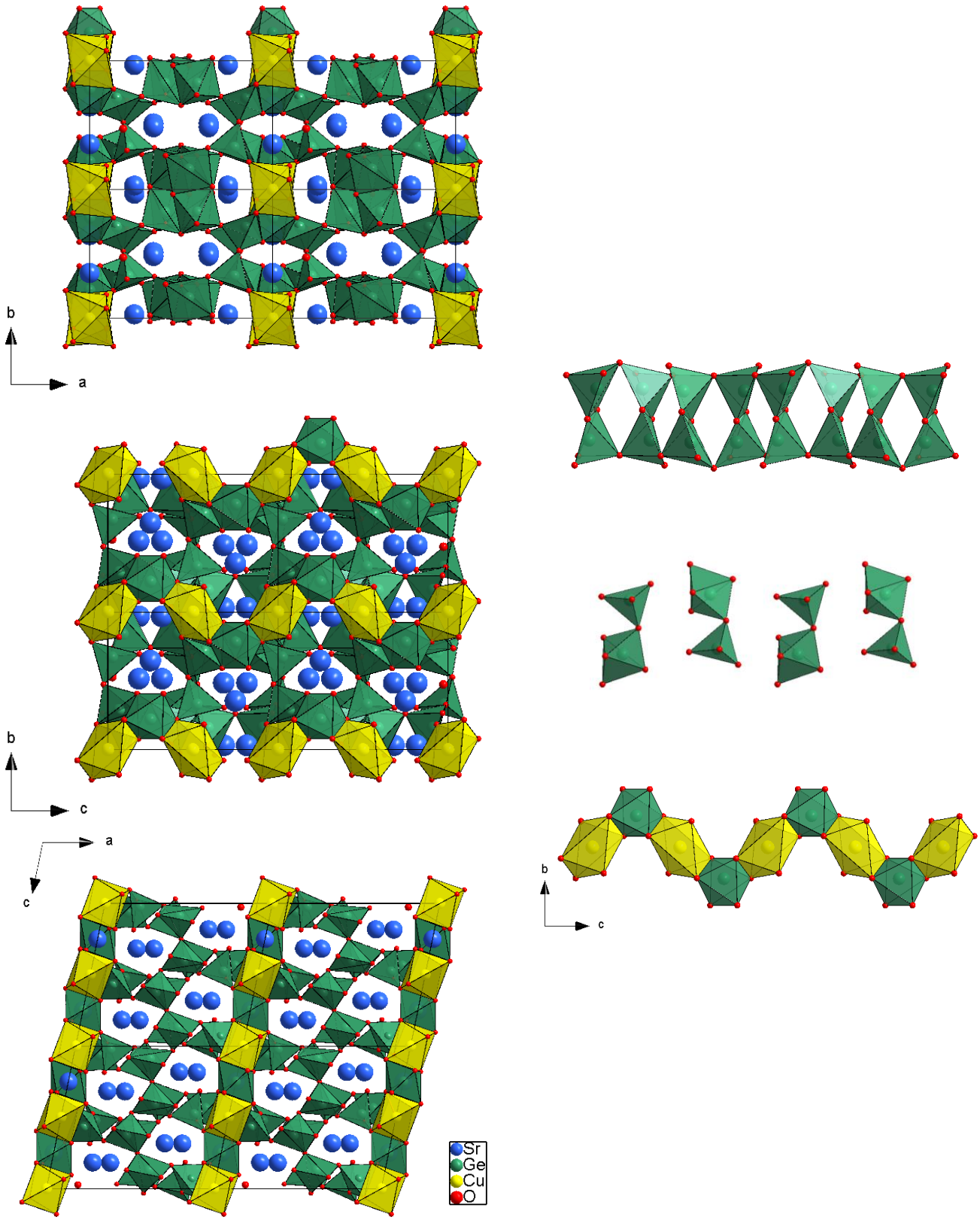

Figure 2: Left: projections along the *c*, *a* and *b* axes from top to bottom, of the refined structure of $Sr_5CuGe_9O_{24}$. Right: the three structural building blocks described in the text.

With nine crystallographically different cation sites, the structure of $Sr_5CuGe_9O_{24}$ is quite complex. As can be seen from the structure plots of figure 2 and the interatomic distances in table 3, it can be described as an arrangement of layers perpendicular to the **a** axis, each layer being composed by a different set of polyhedra chains running along the **c** axis. In this respect, it can be viewed as reminiscent to the structure of pyroxenes and other chain silicates or germanates, but a closer examination reveals its unique character. The x = 0 layer is made of zigzag chains of alternating $Cu1O_6$ and $Ge5O_6$ edge-sharing octahedra. The $Cu1O_6$ octahedra are strongly Jahn-Teller distorted, with four shorter distances at 2.03-2.05 Å forming a distorted square and two long apical ones at 2.67 Å. This leads to a bond valence sum of ca. +1.5 and the absence of magnetic moment for the copper cations. The x = ½ layer is made of chains of edge-sharing Ge_2O_8 pairs of $Ge2O_5$ and $Ge4O_5$ pyramids, the pairs sharing corners to form chains running along the **c** axis. A sixth oxygen anion completes the $Ge2O_5$ and $Ge4O_5$ pyramids at a distance too large to be considered as part of the Ge cation coordination spheres (Ge2-O2 = 2.69 Å and Ge4-O2 = 2.46 Å). The existence of such chains made of corner-sharing Ge_2O_8 bipyramids is quite unique. Similar Ge_2O_8 groups, are observed e.g. in $RCrGeO_5$ (R=Nd–Er, Y) compounds (Shpanchenko *et al*., 2008), but are not connected to form chains. In these two layers, the chains are isolated. The layers are interconnected via corner sharing by pairs of corners-sharing $Ge1O_4$ and $Ge3O_4$ tetrahedra (the coordination of Ge1 could also be considered as a trigonal bipyramid, if one takes into account an additional long Ge1-O13 apical distance at 2.26 Å). The three types of Sr cations are situated inside voids generated by the Cu-Ge-O chain framework in distorted polyhedra with coordination numbers 7, 8 or 9.

The coordination of the Ge cations in $Sr_5CuGe_9O_{24}$ is quite unusual since three different types of coordination polyhedra can be observed. This feature violates Pauling's rule of parsimony which states that "the polyhedra circumscribed about all chemically identical cations should, if possible, be chemically similar" (Pauling, 1929). However, in the present structure, Ge1 and Ge3 are located inside oxygen tetrahedra, Ge2 and Ge4 are five-fold coordinated by oxygen pyramids and Ge5 is surrounded by an oxygen octahedron. In the literature the only oxide phase that is reported to have a similar feature is the form II of $BaGe_2O_5$ (Ozima, 1985). This phase is also monoclinic with a slightly larger unit cell ($P2_1/a$, a = 13.214 Å, b = 13.043 Å, c =9.5501 Å, β = 94.006°). The Ge-oxygen distances compare well to what we find in $Sr_5CuGe_9O_{24}$ except for the tetrahedral environment that is more distorted in $BaGe_2O_5$ (1.73 Å < $d_{Ge\text{-}O}$ < 2.14 Å). Interestingly, this phase was also synthesized under high pressure – high temperature conditions. This might be ascribed to the well-known trend in high pressure phases toward an increase of the number of oxygen neighbors for cations such as Si or Ge.

Table 3: Interatomic distances between the cations and their surrounding oxygen polyhedra.

cation	**anion**	**Distance (Å)**	**cation**	**anion**	**Distance (Å)**
Sr1	**O1 x2**	2.66(3)	**Ge2**	**O2**	1.95(3)
	O3 x2	2.28(2)		**O2**	2.69(3)
	O8 x2	2.44(3)		**O5**	1.82(3)
	O11 x2	3.01(2)		**O6**	1.91(3)
Sr2	**O1**	2.61(3)		**O7**	2.02(3)
	O2	2.52(3)		**O10**	1.83(3)
	O5	2.99(2)	**Ge3**	**O1**	1.70(3)
	O6	2.74(3)		**O4**	1.73(3)
	O6	2.83(3)		**O6**	2.87(3)
	O8	2.69(3)		**O9**	1.67(3)

	O9	2.69(3)		**O11**	1.71(3)
	O10	3.06(3)	**Ge4**	**O2**	2.46(3)
	O13	2.25(2)		**O2**	1.90(3)
Sr3	**O1**	2.47(2)		**O4**	1.90(3)
	O4	2.52(3)		**O5**	1.92(3)
	O5	2.41(3)		**O6**	1.89(3)
	O7	2.48(2)		**O12**	1.84(2)
	O10	2.54(3)	**Ge5**	**O3 x2**	1.91(3)
	O11	2.79(3)		**O9 x2**	1.99(2)
	O12	2.76(2)		**O13 x2**	1.83(3)
Ge1	**O3**	1.96(3)	**Cu1**	**O8 x2**	2.03
	O8	1.62(3)		**O13 x2**	2.05
	O10	1.74(3)			
	O11	1.87(3)			
	O13	2.27(3)			

5. Conclusion

We have shown that the high pressure and high temperature synthesis with the nominal composition $SrCuGe_2O_6$ yields a mixture of a dominant unknown phase and two impurity phases. By combining the EDS analysis and the low-dose electron diffraction tomography, we have identified the unknown phase and successfully solved its complex structure. The obtained model $Sr_5CuGe_9O_{24}$ contains all the atoms of the structure including all oxygens, and the XRPD refinement showed that the precision of the original model is high, confirming also the unusual existence of 3 different coordination numbers for Ge in this phase synthesized under high pressure – high temperature conditions.

References

Burla, M.C., Caliandro, R., Carrozzini, B., Cascarano, G.L., Cuocci, C., Giacovazzo, C., Mallamo, M., Mazzone, A., Polidori, G. (2015) *J. Appl. Cryst*.48 306–309

Colin, C. V, Ding, L., Ressouche, E., Robert, J., Terada, N., Gay, F., Lejay, P., Simonet, V., Darie, C., Bordet, P. & Petit, S. (2020). *Phys. Rev. B.* **101**, 235109.Ding, L., Colin, C. V., Darie, C., & Bordet, P. (2016) *J. Mater. Chem. C*, ***4***(19), 4236–4245.

Ding, L., Colin, C. V., Darie, C., Robert, J., Gay, F., & Bordet, P. (2016) *Phys. Rev. B*, ***93***(6), 064423

Ding, L., Darie, C., Colin, C. V. & Bordet, P. (2016) *Miner. Mag.*, **80**(April), 1–16.

Isobe, M., Ninomiya, E., Vasilev, A.N. and Ueda, Y. (2002) *J. Phys. Soc. Jpn*., **71**, 1423–1426

Jodlauk, S., Becker, P., Mydosh, J.A., Khomskii, D.I., Lorenz, T., Streltsov, S.V., Hezel, D.C. and Bohaty, L. (2007) *J. of Phys.: Cond. Matter*, **19**, 432201–432209

Kim, I., Jeon, G.G., Patil, D., Patil, S., Nenert, G. and Kin, K.H. (2012) *Journal of Physics: Condensed Matter*, **24**, 306001–306007

Kodjikian S. & Klein H. (2019) *Ultramicroscopy*, **200**, 12-19,

Nénert, G., Isobe, M., Kim, I., Ritter, C., Colin, C. V., Vasiliev, A. N., … Ueda, Y. (2010) *Phys. Rev. B*, ***82***(2), 024429

Ozima M., (1985) *Acta Cryst.* **C41**, 1003-1007

Palatinus, L., PETS - Program for analysis of electron diffraction data, Prague: Institute of Physics of the AS CR (2011)

Pauling, L. (1929) *J. Am. Chem. Soc*., **51**, 4, 1010–1026

Petříček, V., Dusek, M., Palatinus, L. (2014) *Z. Kristallogr.* **229** 345-352

Sasago, Y., Hase, M. and Uchinokura, K. (1995) *Phys. Rev. B*, **52**, 3533–3539

Shpanchenko, R. V., Tsirlin, A. A., Kondakova E.S., Antipov, E. V., Bougerol C., Hadermann J., van Tendeloo G., Sakurai H., Takayama-Muromachi E., Journal of Solid State Chemistry 181 (2008) 2433–2441

Tovar, M.;Dinnebier, R.E.;Eysel, W. (1998) *Materials Science Forum* 278, 750-755

Valenti, R., Saha, D.T. and Gros, C. (2002) *Phys. Rev. B*, **66**, 054426

Zheludev, A., Shirane, G., Sasago, Y., Hase, M. and Uchinokura, K. (1996) *Phys. Rev. B*, **53**, 11642